Biochimica et Biophysica Acta 859 (1986) 246–256
Elsevier

BBA 73151

Thermal and structural behavior of natural cerebroside 3-sulfate in bilayer membranes

Martin J. Ruocco and G. Graham Shipley

Biophysics Institute, Departments of Medicine and Biochemistry, Boston University School of Medicine, Housman Medical Research Center, 80 East Concord Street, Boston, MA 02118 (U.S.A.)

(Received February 12th, 1986)

Key words: Sulfatide; Cerebroside; Bilayer structure; Hydration; Myelin; Differential scanning calorimetry; X-ray diffraction; Polarizing microscopy; (Bovine brain)

Differential scanning calorimetry (DSC), polarizing microscopy and X-ray diffraction studies have been performed on dry and hydrated natural bovine brain sulfatides. Dry sulfatide fractions exhibit a high temperature transition (ΔH = 6.6 kcal/mol sulfatide) at 87.3°C. X-ray diffraction shows this transition to be associated with a hydrocarbon chain order-disorder transformation between two lamellar phases. Hydrated sulfatide dispersions undergo a complex chain order-disorder transition (ΔH = 7.5 kcal/mol sulfatide) at 32°C with two peak temperatures at 35°C and 47°C. Structural studies performed on hydrated liquid-crystal sulfatide dispersions at 75°C verify the existence of a bilayer structure over the 16 wt.% to 50 wt.% phosphate buffer (pH = 7.4) range. The intrabilayer separation between galactosyl-3-sulfate groups averages 48 Å as the multilamellar bilayers swell with the addition of phosphate buffer. The formation of micellar phases is not observed at high water contents. The comparison of the structural characteristics of dry and hydrated sulfatides with structural data for dry and hydrated bovine brain non-sulfated glycolipid (cerebroside) is discussed in molecular terms.

Introduction

Integral structural and/or functional roles for the galactosphingolipids, galactocerebroside and galactocerebroside sulfate (sulfatide), in the central and peripheral nervous systems have been implicated in recent years. For example, cerebrosides, which constitute the major proportion of peripheral and central nervous system galactolipids, are important for normal myelination during early brain development [1], and myelin function. In certain diseases (e.g. Pelizaeus-Merzbacher), where the scarcity or total absence of galactocerebroside results in defective nerve conduction, the importance of cerebroside is accentuated [2]. In dysmyelinating diseases such as Krabbe's [3,4], and metachromatic leucodystrophy [5] there is an accumulation of galactocerebroside and sulfatide, respectively.

Galactocerebroside is the major neutral galactosphingolipid in myelin and has been studied by a number of physical techniques including X-ray crystallographic [6], powder X-ray diffraction [7,8], monolayer [9–11], and thermal methods [8,12–14].

Sulfatides constitute the minor galactosphingolipid of the nervous system. As in the case of cerebroside, sulfatide contains both non-hydroxy and hydroxy acyl chains. The proportions of hydroxy fatty acid-sulfatide varies between 20 and 60 percent of the total sulfatide fraction [15,16]. The sulfoglycosphingolipid is suggested to be associated in an undefined manner with opiate (endorphin) receptor binding [17], and specific neurotransmitter responses [18]. In both the nervous

0005-2736/86/$03.50 © 1986 Elsevier Science Publishers B.V. (Biomedical Division)

system and non-neural tissues sulfatide is implicated as having a specific role in sodium and potassium ion transport where sulfatide concentration is correlated with both Na^+- and K^+-ATPase activity and sodium flux across membranes [19]. In contrast to cerebrosides, natural and semi-synthetic sulfatides have only recently been characterized by a few physical methods. For example, turbidometric and monolayer studies have assessed the binding affinities of cations to sulfatides [20,21]. Recently, the calorimetric behavior of natural non-hydroxy and hydroxy fatty acid sulfatide fractions, as well as semi-synthetic sulfatides with specific *N*-acyl chains, has been characterized [22,23]. There is little structural data available, however, for natural and/or semi-synthetic sulfatide dispersions to date (see, for example, Ref. 7).

In this report we present thermal and structural data for dry and hydrated natural whole fraction sulfatides utilizing polarizing microscopy, differential scanning calorimetry (DSC), and X-ray diffraction.

Materials and Methods

Natural lipid extracts of bovine brain cerebroside sulfate (sulfatide), as the sodium salt (Na^+-sulfatide) and brain cerebroside were obtained from Supelco (Bellefonte, PA). The cerebrosides and sulfatides gave two spots by thin-layer chromatography using chloroform/methanol/water/acetic acid (65 : 25 : 4 : 1, v/v) as eluting solvent and were used without further purification. The fatty acid compositions of the glycosphingolipids were determined by gas-liquid chromatography and are given in Table I.

TABLE I

FATTY ACID COMPOSITIONS OF THE GLYCOSPHINGOLIPIDS

Fatty acid	Bovine brain sulfatide (%)	Bovine brain cerebroside (%)
16:0	–	0.24
18:0	3.30	1.72
20:0	0.75	0.26
22:0	8.17	1.56
24:1	7.45	1.27
23:0	3.86	–
24:0	23.20	4.71
25:1	0.74	–
25:0	4.37	–
26:1	2.60	–
15:0/OH	–	0.02
18:0/OH	5.75	21.06
19:0/OH	0.47	1.05
20:0/OH	0.18	0.85
23:0/OH	3.19	6.44
22:0/OH	4.22	8.19
24:1/OH	2.73	5.05
24:0/OH	18.72	32.21
25:1/OH	–	2.51
25:0/OH	2.78	5.19
26:1/OH	2.50	3.85
26:0/OH	2.00	2.95
25:1/OH	2.37	–
25:0		

Sample preparation

Sulfatides were used directly as the dry powder. Dry samples were taken for polarizing light microscopy, differential scanning calorimetry, and X-ray diffraction.

For the hydrated preparations, sulfatides were weighed gravimetrically into a tube having a narrow constriction in the middle, the appropriate quantity of double distilled water or buffer was introduced by microsyringe below the constriction, the tube flushed with nitrogen below the constriction, and then flame-sealed above the constriction. For swelling experiments, the buffer 0.05 M sodium phosphate (pH 7.4)/0.15 M NaCl was used. The samples were equilibrated by repeated centrifugation of the dispersion through the constriction until the dispersion was visually homogeneous at a temperature above T_m. After equilibration the constricted tubes were opened, immediately mixed and the well-mixed aliquots taken for polarizing microscopy, DSC and X-ray diffraction. In some instances, lipid mixtures were prepared directly into DSC pans and equilibrated by centrifuging the DSC pans at the appropriate temperature. Consistent and reproducible behavior was obtained with both methods of equilibration.

Polarizing microscopy

An aliquot of dry neat lipid or pre-equilibrated, hydrated lipid dispersion was placed on a microscope slide, covered with a coverslip, and sealed at the edges with epoxy resin. Samples were examined by direct and polarizing light with a Zeiss NL microscope fitted with a heating/cooling stage. Changes in optical texture and sample viscosity were determined during heating and cooling in the temperature range 20°C to 200°C for anhydrous lipid samples and from 20°C to 90°C for hydrated lipid dispersions.

Differential scanning calorimetry

Hydrated samples (1–15 mg) prepared as described above were hermetically sealed in stainless steel DSC pans. In other experiments, dry sulfatides were weighed into the DSC pan and the appropriate amount of doubly distilled water or buffer added. The pans were hermetically sealed. Heating and cooling scans over the temperature range 20°C to 90°C were performed on a Perkin-Elmer DSC-2 scanning calorimeter (Norwalk, CT) using heating/cooling rates of 5 K/min. Isothermal modes were also utilized. Transition temperatures were determined from the onset of the transition extrapolated to the baseline. Enthalpy measurements were determined from the area under the transition peak by comparison with those for a known standard (gallium). Baselines in the region of the transition were approximated by extrapolating the pre-transition baseline to the post-transition baseline.

X-ray diffraction

Hydrated sulfatide samples were transferred to 1 mm (inner diameter) capillaries (Charles Supper Co., Natick, MA). The capillary tubes were flame-sealed and placed in a sample holder kept at constant temperature by a circulating solvent/water bath. Nickel-filtered CuK_α X-radiation ($\lambda = 1.5418$ Å) from an Elliot GX-6 rotating anode X-ray generator (Elliot Automation, Borehamwood, U.K.) was point-focused by either a toroidal mirror optical camera or a double-mirror optical camera. Diffraction patterns were recorded on Kodak No-Screen X-ray film.

X-ray diffraction data were also recorded using a position-sensitive detector counter method. Nickel-filtered CuK_α X-radiation was produced from a microfocus X-ray generator (Jarrell-Ash, Waltham, MA), line-focused by a single mirror and collimated using the slit optical system of a Luzzati-Baro camera. X-ray diffraction data were recorded using a linear position-sensitive detector (Tennelec, Oak Ridge, TN) and associated electronics (Tracor Northern, Middleton, WI). In all cases, samples were contained in thin-walled capillary tubes (internal diameter 1.0 mm) and mounted in variable temperature sample holders. Temperature stability was ± 0.5 K.

Results

Dry bovine brain sulfatide

Polarizing microscopy

Dry bovine brain sodium sulfatide is a fine white powder at 22°C. By polarizing microscopy, the sulfatide remains in the white powder form until temperatures > 87°C are reached. Above 87°C a 'neat' phase, non-geometrical, waxy texture [24] is found indicative of a lamellar structure (Figs. 1A and 1B). This texture is brittle at temperatures between 87°C and 127°C. At 127°C an isotropic liquid is observed (Fig. 1C). In contrast to bovine brain cerebroside [14], textures characteristic of the hexagonal 'middle' phase (e.g. striations, see Ref. 24) are not observed in the sulfatide liquid crystal.

Differential scanning calorimetry

The calorimetric behavior of dry sulfatide is summarized in Fig. 2. The initial heating scan over the 20°C to 100°C range demonstrates a single endothermic transition at 87.3°C with an enthalpy of 6.6 kcal/mol sulfatide (Fig. 2A). Cooling from 100°C results in a single exotherm ($\Delta H = 6.6$ kcal/mol) at 87.3°C. Further heating to 127.3°C yields a low enthalpy transition, $\Delta H = 0.8$ kcal/mol (Fig. 2C). This thermal behavior is totally reproducible provided the sample is not heated to temperatures greatly exceeding the 127°C liquid-crystal → isotropic liquid transition. Prolonged periods at these higher temperatures results in chemical degradation of the sulfatide.

X-ray diffraction

X-ray diffraction experiments were performed

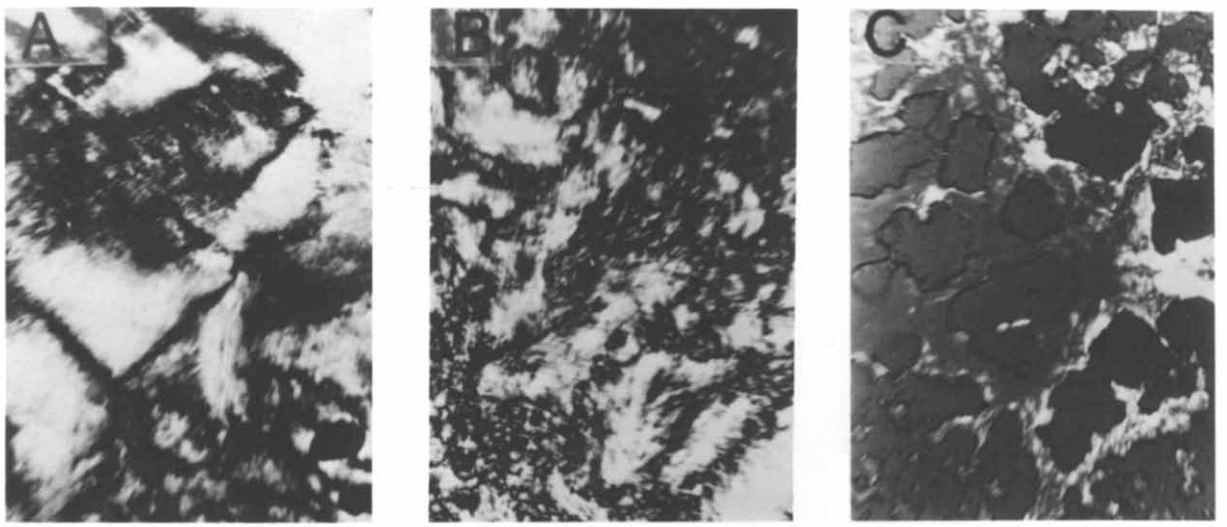

Fig. 1. Polarizing light microscopy of dry bovine brain sulfatide. Non-geometrical texture at 100°C (A) and at 120°C (B). (C) Isotropic liquid and liquid crystal at the isotropic liquid ↔ liquid-crystal transition, 130°C.

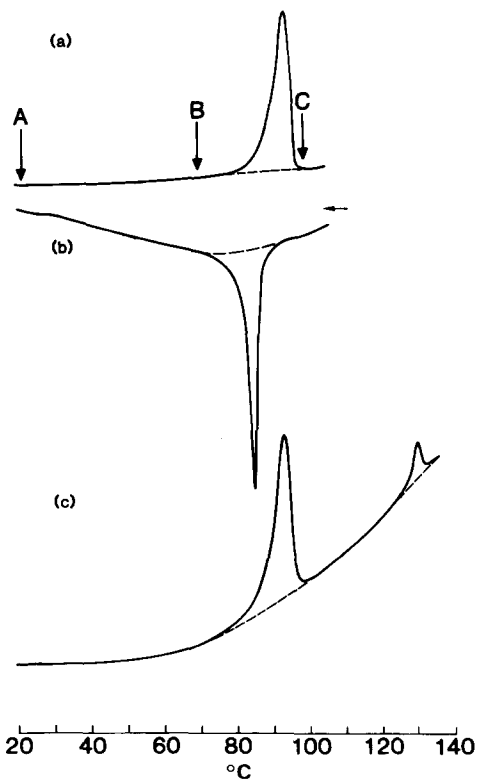

Fig. 2. DSC thermograms of dry bovine brain sulfatide. (a) heating scan; (b) cooling scan; (c) immediate reheating scan; programming rate = 5 K/min. Lettered arrows correspond to X-ray diffraction patterns in Figure 3.

at temperatures corresponding to the lettered arrows in Fig. 2A and the diffraction patterns are shown in Fig. 3.

The X-ray diffraction pattern of bovine brain sulfatide at 22°C demonstrates five orders of reflections indexing on a lamellar geometry with a periodicity of 67.1 Å. Only a single, strong wide-angle reflection occurs at 1/4.04 $Å^{-1}$ (Fig. 3A). This diffraction pattern should be contrasted with that of dry whole fraction bovine brain cerebrosides which exhibits seven orders of lamellar reflections ($d = 47.6$ Å) and wide-angle reflections at 1/4.5, 1/4.1 and 1/3.7 $Å^{-1}$ (Fig. 4). Heating to 70°C, a temperature just below the sulfatide crystal → liquid-crystal mesophase transition (see Fig. 2A), yields the diffraction pattern shown in Fig. 3B. The lamellar periodicity of the high-temperature gel form is reduced to 65.3 Å. The wide-angle region still exhibits only a single reflection, although this reflection is sharper than that of the corresponding low-temperature form and occurs at a slightly larger spacing, 1/4.15 $Å^{-1}$ (compare Figs. 3A and 3B). The diffraction pattern shown in Fig. 3C was recorded at 96.6°C, a temperature above the large enthalpy transition at 87.3°C. This diffraction pattern demonstrates that the liquid crystal has a lamellar geometry with a reduced periodicity of 57.7 Å. Strong first- and

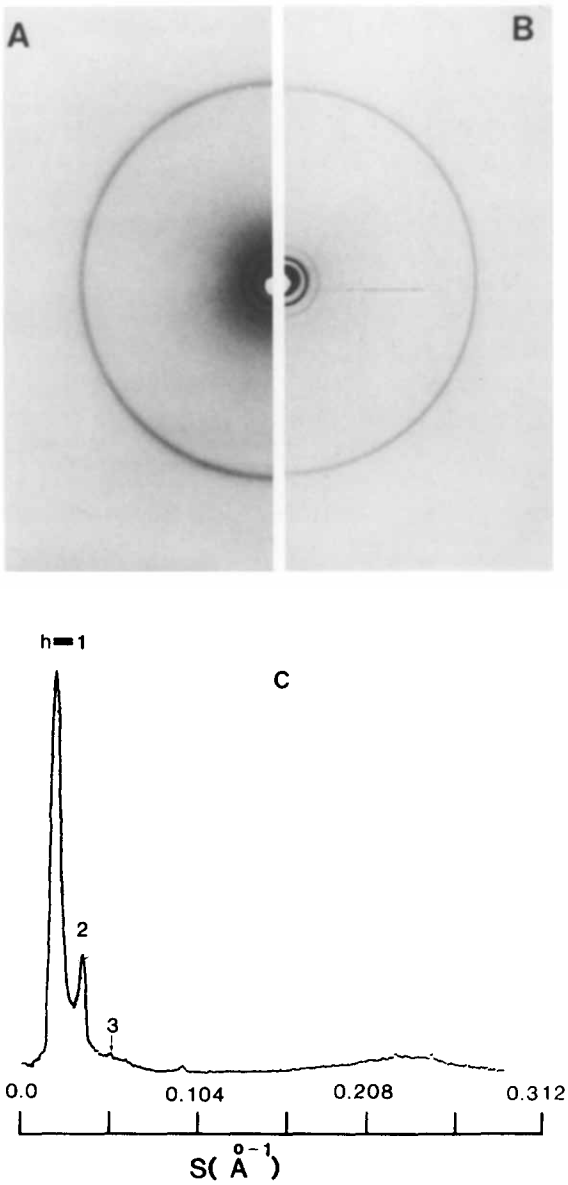

Fig. 3. X-ray diffraction patterns of dry bovine brain sulfatide at (A) 22°C; (B) 70°C and (C) 96.6°C; the X-ray diffraction pattern in (3C) was recorded using a position-sensitive detector.

second-order reflections are readily apparent with a weak third-order reflection at $1/19.2$ Å^{-1}. The single broad wide angle reflection occurs at $1/4.6$ Å^{-1}. which is characteristic of the disordered hydrocarbon chain packing.

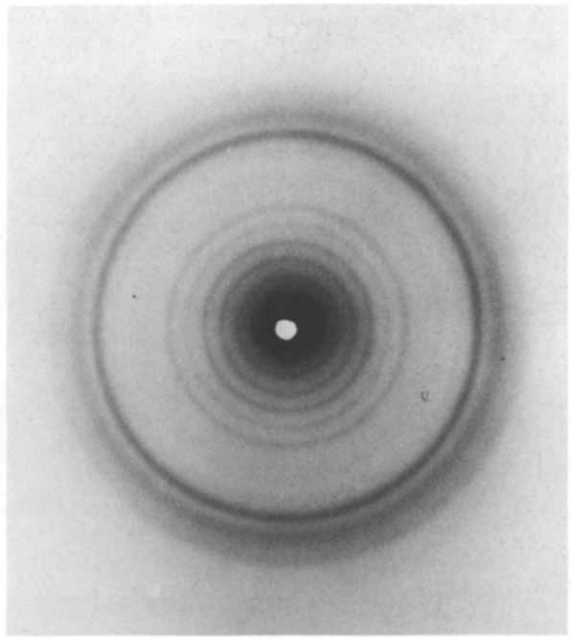

Fig. 4. X-ray diffraction pattern of dry bovine brain cerebroside at 22°C.

Hydrated bovine brain sulfatide

Polarizing microscopy

Sulfatide dispersions containing low (35 wt.% H_2O) and high (70 wt.% H_2O) water contents were examined under the polarizing microscope over the temperature range 20°C to 80°C. At 20°C both samples demonstrate a 'neat' phase mosaic texture [24]. The mosaic textures observed at low and high hydration flow easily. On heating to 70°C, the texture remains similar to that found at lower temperatures, a 'neat' phase mosaic texture. In addition, focal conics having a positive sign of birefringence are observed (Fig. 5). Other textures observed at water contents greater than 70 wt.% H_2O at 70°C include oily streaks and myelin figures [24]. Only textures characteristic of lamellar phases are observed and no textures suggestive of hexagonal 'middle' phase were present.

Differential scanning calorimetry

The calorimetric behavior of a 43 wt.% H_2O dispersion is summarized in Fig. 6. The initial

Fig. 5. Polarizing light microscopy of hydrated (> 70 wt.% water) bovine brain sulfatide at 70°C. A neat phase mosaic texture with oily streaks and focal conics is observed.

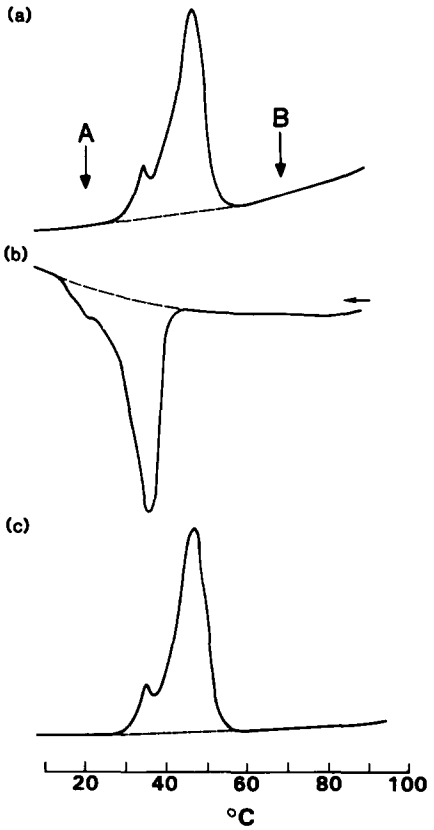

Fig. 6. DSC thermograms of hydrated (43 wt.% water) bovine brain sulfatide. (a) initial heating scan; (b) cooling scan; (c) immediate reheating scan; programming rate = 5 K/min. Lettered arrows correspond to X-ray diffraction patterns in Fig. 7.

heating scan demonstrates a broad endotherm at 31.8°C with peak maxima at 34.8°C and 47.3°C. The total enthalpy of the transition is 7.5 kcal/mol sulfatide. On cooling from 90°C an exotherm ($\Delta H = 7.5$ kcal/mol) is observed. Subsequent reheating to 90°C results in the reappearance of the double-peaked endotherm. Calorimetric thermograms of sulfatide at greater hydrations (i.e. > 70 wt.% H_2O) demonstrated similar behavior.

X-ray diffraction

The X-ray diffraction patterns for a 43 wt.% H_2O sample are shown in Fig. 7. At 22°C, the diffraction pattern indexes as a lamellar geometry with a large periodicity of 102.7 Å (Fig. 7A). (Note that the primary reflection is behind the lead back stop with this geometry). The wide-angle reflection at 1/4.18 $Å^{-1}$ is relatively diffuse compared to the dry sulfatide diffraction pattern at 22°C (compare with Fig. 3A). As in the case of dry whole bovine brain cerebrosides (see above), hydrated cerebroside bilayers exhibit a diffraction pattern ($d = 65.2$ Å) indicative of greater order compared to sulfatides as evidenced by several reflections in the $1/10 < 1/d < 1/3$ $Å^{-1}$ region (compare Figs. 7 and 8). Heating sulfatide through the gel → liquid-crystal transition at 32°C to 70°C yields a second lamellar form with a reduced periodicity of 77.4 Å (Fig. 7B). The diffuse wide-angle spacing at 1/4.5 $Å^{-1}$ is reflective of the greater hydrocarbon chain disorder relative to the gel lamellar form.

X-ray diffraction studies of bovine brain sulfatide were performed as a function of water content at a temperature above the gel → liquid-crystal transition (75°C). Fig. 9 shows the X-ray diffrac-

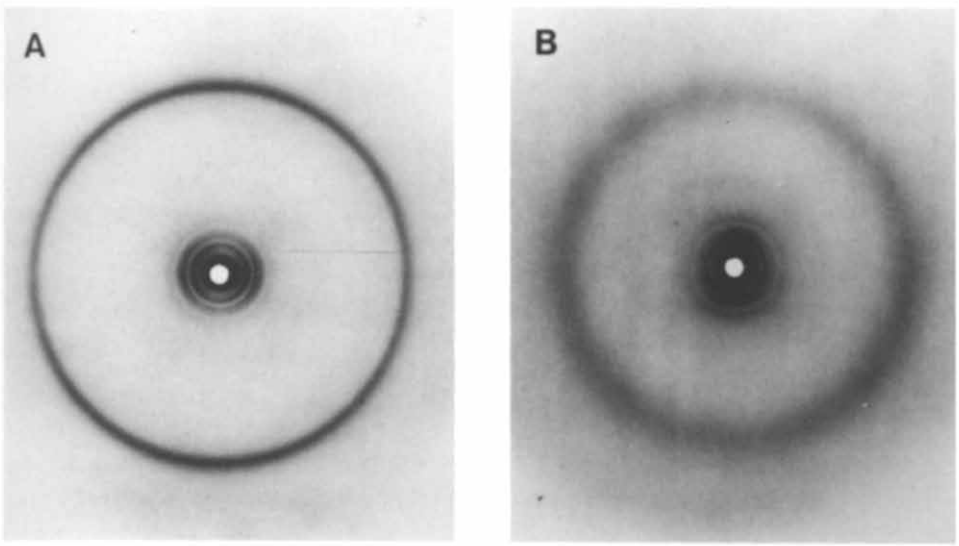

Fig. 7. X-ray diffraction patterns of hydrated (43 wt.% water) bovine brain sulfatide at (A) 22°C and (B) 70°C.

tion patterns from sulfatide dispersions containing 16.4 wt.% to 41.1 wt.% phosphate buffer. Only the low-angle region of the X-ray diffraction patterns

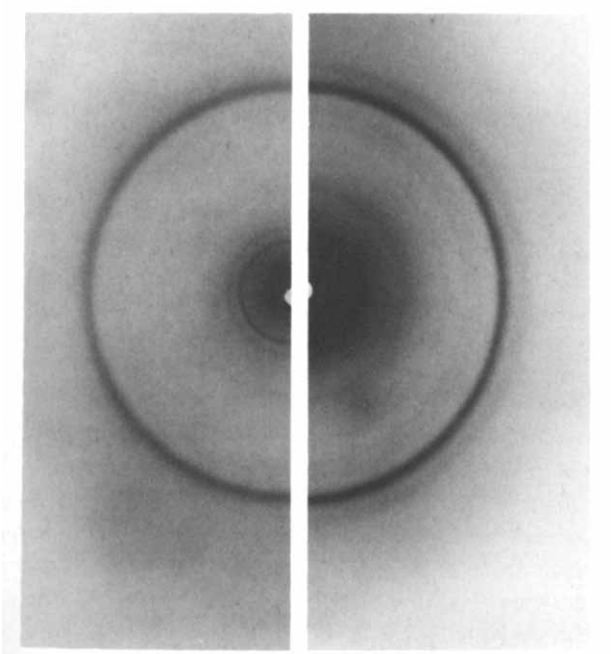

Fig. 8. X-ray diffraction pattern of hydrated (70 wt.% water) bovine brain cerebroside at 22°C. Exposures were under- (left) and overexposed (right) to accentuate the low-angle and wide-angle reflections, respectively.

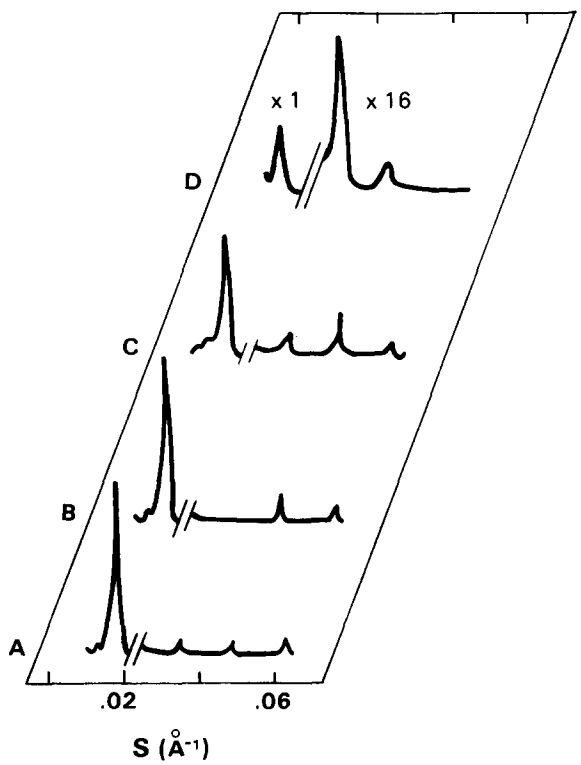

Fig. 9. X-ray diffraction patterns, recorded with a linear position-sensitive detector, of bovine brain sulfatide/buffer dispersions. (A) 16.4; (B) 20.9; (C) 26.0; (D) 41.1 wt.% buffer at $T = 75°C$. Buffer: 0.05 M sodium phosphate/0.15 M sodium chloride (pH 7.4).

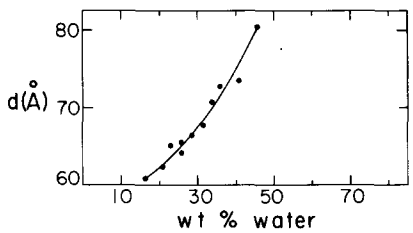

Fig. 10. Lamellar spacing (d) for bovine brain sulfatide/buffer dispersions as a function of wt.% buffer at $T = 75°C$. Buffer: 0.05 M sodium phosphate/0.15 M sodium chloride (pH 7.4).

(i.e. $1/d < 1/10$ Å^{-1}) is shown in this figure. Note the variation in the position, number and intensity of the lamellar reflections. Fig. 10 summarizes the changes in lamellar periodicity, d, as a function of hydration. The periodicity increases continuously from $d = 61.5$ Å (16.4 wt.% buffer) to 80.5 Å (45.8 wt.% buffer). The normalized, observed structure factor amplitudes $F(s)$, for the series of low-angle reflections at various hydrations are plotted as a function of s ($2 \sin \theta/\lambda$)) in Fig. 11 to give the continuous transform. From the phased $F(s)$, one-dimensional electron-density profiles of Na^+-sulfatide bilayer dispersions were obtained. Fig. 12 depicts representative electron-density profiles of bilayers containing 16.4, 28.8, 36.4 and 45.8 wt.% buffer. The assigned phases are indicated in Fig. 12. The electron density profiles are characterized by two peaks corresponding to the electron-dense sugar groups separated by a low electron density trough corresponding to the bilayer center. Clearly the bilayer thickness as measured by the separation of the sugar moieties does not change significantly with increasing hydration ($d_{GG} = 47$–49 Å). The precise shape of the trough is influenced by the progressively lower resolution of the profile (4 → 3 reflections) as the

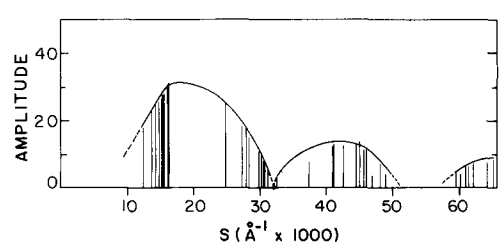

Fig. 11. Structure factor amplitude curve for bovine brain sulfatide/buffer bilayer dispersions at $T = 75°C$. Buffer: 0.05 M sodium phosphate/0.15 M sodium chloride (pH 7.4).

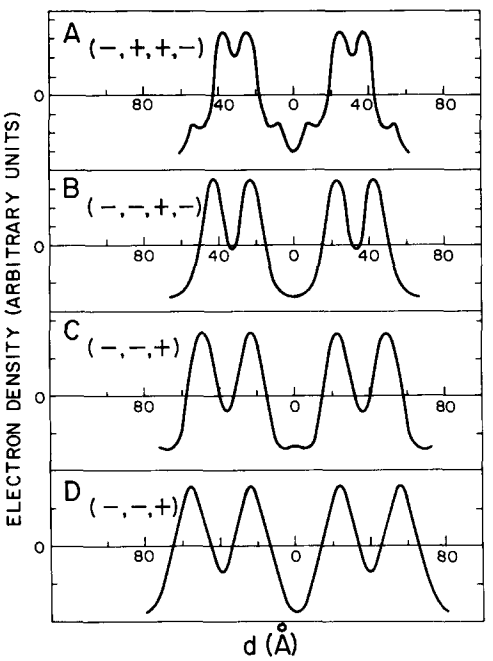

Fig. 12. One-dimensional electron density profiles of bovine brain sulfatide bilayers at $T = 75°C$ containing (A) 16.4; (B) 28.8; (C) 36.4; (D) 45.8 wt.% buffer. Buffer: 0.05 M sodium cholate/ 0.15 M sodium chloride (pH 7.4).

bilayer periodicity increases (61.5 → 80.5 Å) with hydration.

Discussion

Comparison of the dry sulfatide diffraction pattern at 22°C (Fig. 3A) with the diffraction pattern of dry bovine brain cerebroside at 22°C (Fig. 4) clearly indicates structural and packing differences between the sulfatide and cerebroside bilayers. The large number of wide angle spacings in the cerebroside diffraction pattern is suggestive of a more ordered, complex hydrocarbon chain packing mode compared to the hexagonal-type chain packing of sulfatide which is characterized by less specific chain-chain contacts [25]. From a chemical viewpoint, the addition of the SO_3^- group to the 3-position of the galactose moiety provides a bulky charged group which, in addition to the electrostatic repulsion between adjacent negatively-charged sulfatides, should create a larger surface area per headgroup. Hence, the surface area per molecule would be expected to be larger

than the non-sulfated cerebroside. The negatively-charged $-SO_3^-$ and the increased area per sulfatide not only allows less specific interchain contact which results in a non-specific chain-chain packing mode but probably hinders the establishment of an ordered polar-interfacial lattice characteristic of cerebroside bilayers [6].

The neat liquid-crystal phase at 96°C (see Fig. 3C) is also lamellar, having a reduced periodicity of 57.7 Å. This is to be contrasted with the cerebroside liquid-crystal which exhibits middle phase textures and probably forms a non-lamellar structure [8,14].

The combined calorimetric and X-ray diffraction data show that bovine brain sulfatide forms a hydrated lamellar gel (Figs. 6 and 7) at temperatures below 31.8°C for all water concentrations studied. The gel undergoes a hydration-dependent reproducible gel → liquid-crystal transition at the limiting temperature of 31.8°C to a liquid-crystal lamellar form (Fig. 6). In both the gel and liquid-crystal states bovine brain sulfatide is shown to take up water continuously over the 20 to 50 wt.% buffer hydration range. This is in contrast to the hydrated palmitotylcerebroside, bovine brain non-hydroxy fatty acid cerebroside and whole fraction cerebroside crystal and liquid-crystal bilayers which exhibit no or limited swelling behavior (< 20 wt.% H_2O) for the crystal at 22°C and the liquid crystal at 90°C [14,26].

The one-dimensional electron density profiles of hydrated liquid-crystal Na^+-sulfatide dispersions indicate a bilayer structure over the 16.4 to 45.8 wt.% aqueous buffer concentration range. The bilayer thickness, d_{GG}, decreases only slightly as hydration is increased to an average value of $d_{GG} \approx 47.5$ Å over the 36 to 50 wt.% buffer range (see Table II). The relatively constant d_{GG} versus an increasing lamellar periodicity, d, indicates, as depicted in the one-dimensional electron density profiles, that there is a continuously increasing interbilayer separation as more aqueous buffer is added to the bilayer dispersion.

The lamellar nature of hydrated bovine brain sulfatide has been established by combined polarizing microscopy and X-ray diffraction up to 50 wt.% H_2O. Diffraction data beyond 50 wt.% H_2O are limited due to the diffuse nature of the Bragg spacings as a result of multilayer stacking

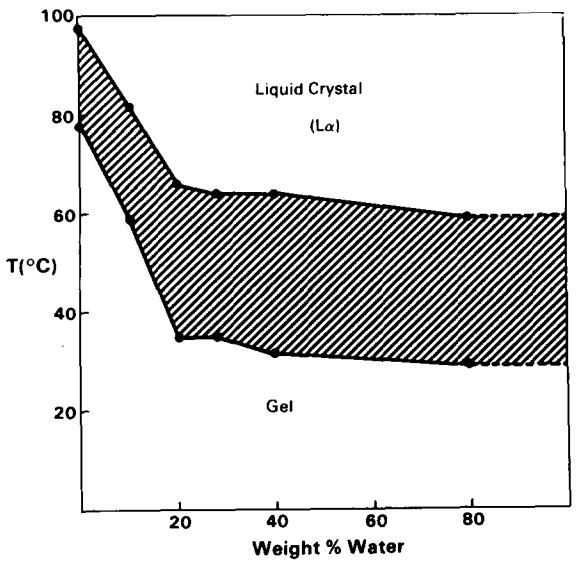

Fig. 13. Temperature-composition phase diagram of bovine brain sulfatide-water system based on DSC data.

disorder. Polarizing microscopy of dispersions containing > 70 wt.% H_2O at 20°C and 70°C (Fig. 5), however, demonstrate optical activity characteristic of a neat phase (mosaic texture with focal conics having a positive sign of birefringence). This is clearly indicative of a lamellar liquid-crystal phase. At high water concentrations (> 90 wt.% H_2O), dispersions of sulfatide demonstrate turbidity and are not clear solutions as expected for micellar solutions at temperatures over the 20°C to 80°C range. Based on these observations, polarizing microscope textures, calorimetric data and diffraction data, the phase diagram for hydrated sulfatide is constructed (Fig. 13). For the Na^+-sulfatide/water binary system in the 20 to 90°C temperature range, two single-phase zones exist: a continuously swelling lamellar gel (at temperatures $T < T_c$) and liquid crystal (at temperatures $T > T_c$). This behavior is at variance with that reported by Abrahamsson et al. [7] for Na^+-sulfatide derived from human brain. These authors report the formation of a micellar solution at low temperatures for water concentrations (> 70 wt.% H_2O).

The surface area per sulfatide molecule in liquid-crystal bilayers at 75°C is listed in Table II. The surface area per Na^+-sulfatide over the 16.4 to 45.8 wt.% buffer range (64 $Å^2$–67 $Å^2$) is larger

than that obtained for bovine brain cerebroside bilayers at maximum hydration ($S_l = 55$ Å^2; Ref. 7). This increased surface area is clearly reflective of the net negative charge of the sulfate group at the 3-position of the galactosyl headgroup.

As discussed in the case of the anhydrous cerebroside and sulfatide bilayers, the X-ray diffraction data indicate that cerebroside forms a more ordered hydrated bilayer membrane compared to sulfatide bilayers as evidenced by the lack of reflections in the $1/10 < 1/d < 1/3$ Å^{-1} region of the hydrated sulfatide bilayer diffraction patterns (compare Figs. 7 and 8). Although the particular cerebroside fraction used in this study contains a much larger proportion of hydroxylated fatty acids than the sulfatide fraction (Table I), this observation, i.e. several reflections in the $1/10 < 1/d < 1/3$ Å^{-1}, is general for any cerebroside fraction including non-hydroxy fatty acid-rich cerebroside fractions [14]. The ratio of non-hydroxy to hydroxy fatty acid appears not to affect the fact that cerebrosides exhibit X-ray diffraction patterns indicative of more ordered gel bilayers than sulfatide bilayers. Reflections in the $1/10 < 1/d < 1/3$ Å^{-1} region are generally indicative of an ordered two-dimensional packing arrangement in the plane of the bilayer which is attributed to the lipid hydrocarbon chains and may result from ordering at the headgroup-interface region due to packing constraints imparted by a hydrogen bonding matrix. These data, when considered in light of the chemical difference between sulfatide and cerebroside, strongly suggest that both the additional surface area necessary to accommodate the bulky sulfate group and counter ion into the interface region and the electrostatic repulsion of adjacent sulfatide molecules preclude or inhibit the establishment of an extensive, ordered hydrogen bonding network, and consequently, an ordered hydrocarbon chain packing mode as found in the case of cerebroside [6,8]. In effect, the specific area requirements and intermolecular contacts necessary for effecting an ordered interfacial packing are disrupted in the case of both dry and hydrated sulfatide due to the presence of the SO_3^- group, although shielding of the charge by higher concentrations of bound monovalent or divalent cations may counter this effect.

We have suggested that the establishment of a hydrogen bonding network at the headgroup-interface region of the cerebroside translates order along the molecule into the bilayer in the form of closer interchain contact, yielding a more regular intra- and intermolecular packing [8,14]. The absence of such interactions in sulfatide bilayers is reflected in the reduced temperature and enthalpy of the gel bilayer → liquid-crystal bilayer transition (T_M (sulfatide) = 47°C (peak of main transition, Fig. 6) vs. T_M (cerebrosides) = 67°C) (Ref. 13; Ruocco, M.J., unpublished observations). No metastable states were observed under the experimental conditions used to characterize the thermal behavior of sulfatide dispersions. Interestingly, however, metastable states have been reported to occur in semi-synthetic palmitoyl-, stearoyl- and lignoceroyl-sulfatide bilayers [23]. The absence of metastable forms in the whole fraction sulfatide dispersions as studied under conditions used by us may be related to acyl chain heterogeneity (see also Ref. 22).

The swelling behavior of sulfatide is an important factor under pathological conditions (e.g. metachromatic leucodystrophy). Under these conditions abnormally large amounts of sulfatides accumulate in myelin. This accumulation of lipid in effect results in an increase in charge per surface area of myelin which probably allows an increase in average surface area per lipid molecule and an increased uptake of intermembrane water (swelling). Both phenomena result in the malfunction of myelin and dysmyelination.

Although sulfatide occurs in relatively small amounts, its presence and interaction with the cerebroside and phospholipid components of

TABLE II

SURFACE AREA PER MOLECULE SULFATIDE IN LIQUID-CRYSTAL BILAYERS

Buffer: 0.05 M sodium phosphate/0.15 M sodium chloride (pH 7.4).

Wt.% buffer	d_{GG} (Å)	S_l (Å^2)
16.4	49	64
28.8	48	65
36.4	47	67
45.8	48	65

myelin is yet to be fully considered. While it is known that cerebroside has a finite solubility in phospholipid bilayers [27], the miscibility of sulfatide in cerebroside and/or phospholipid in the presence and absence of cholesterol and various types and concentrations of ions is yet to be systematically characterized.

Acknowledgements

We wish to thank Dr. William Curatolo for useful discussions and Dr. Firoze Jungalwala at the Eunice Kennedy Shriver Center for the fatty acid analyses of the sulfatide and cerebroside fractions. This research was supported by research grant HL-26335 and training grants HL-07291 and HL-07429 from the National Institutes of Health.

References

1 Bologa-Sandru, L., Zalc, B., Herschkowitz, N. and Baumann, N. (1981) Brain Res. 225, 425–430
2 Witter, B., Debuch, H. and Klein, H. (1980) J. Neurochem. 34, 957–962
3 Suzuki, K., Tanaka, H. and Suzuki, K. (1976) Adv. Exp. Med. Biol. 68, 99–114
4 Ida, H., Umezawa, F., Kasai, E., Eto, Y. and Maekawa, K. (1982) Biochem. Biophys. Res. Commun. 109, 634–638
5 Dulaney, J.T. and Moser, H.W. (1978) in The Metabolic Basis of Inherited Disease (Stanbury, J.B., Wyngaarden, J.B. and Fredrickson, D.S., eds.), pp. 770–809, McGraw-Hill, New York
6 Pascher, I. and Sundell, S. (1977) Chem. Phys. Lipids 20, 175–191
7 Abrahamsson, S., Pascher, I., Larsson, K. and Karlsson, K.-A. (1972) Chem. Phys. Lipids 8, 152–179
8 Ruocco, M.J., Atkinson, D., Small, D.M., Skarjune, R.P., Oldfield, E. and Shipley, G.G. (1981) Biochemistry 20, 5957–5966
9 Abrahamsson, S., Dahlen, B., Lofgren, H., Pascher, I. and Sundell, S. (1976) in Structure of Biological Membranes (Abrahamsson, S. and Pascher, I. eds.), pp. 1–23, Plenum Press, New York
10 Poss, A., Vancraenbroeck, Berliner, C. and Ruysschaert, J.M. (1979) J. Colloid Interface Sci. 70, 124–129
11 Maggio, B., Cumar, F.A. and Caputto, R. (1981) Biochim. Biophys. Acta 650, 69–87
12 Freire, E., Bach, D., Correa-Freire, M., Miller, I. and Barenholz, Y. (1980) Biochemistry 19, 3662–3665
13 Curatolo, W. (1982) Biochemistry 21, 1761–1764
14 Ruocco, M.J. (1983) Ph.D. Dissertation, Boston University, Boston, MA
15 O'Brien, J.S., Fillerup, D.L. and Mead, J.F. (1964) J. Lipid Res. 5, 109–116
16 Svennerholm, L. and Stallberg-Stenhagen, S. (1968) J. Lipid Res. 9, 215–225
17 Craves, F.B., Zalc, B., Leybin, L., Baumann, N. and Loh, H.H. (1980) Science 207, 75–76
18 Tocque, B., Albouz, S., Boutry, J-M., Le Saux, F., Hauw, J.-J., Bourdin, R., Baumann, N. and Zalc, B. (1984) J. Neurochem. 42, 1101–1106.
19 Zambrano, F., Morales, M., Fuentes, N. and Rojas, M. (1981) J. Membrane Biol. 63, 71–75
20 Abramson, M.B., Katzman, R., Curci, R. and Wilson, C.E. (1967) Biochemistry 6, 295–304
21 Abramson, M.B. and Katzman, R. (1968) Science 161, 576–577
22 Koshy, K.M. and Boggs, J.M. (1983) Chem. Phys. Lipids 34, 41–53
23 Boggs, J.M., Koshy, K.M. and Rangaraj, G. (1984) Chem. Phys. Lipids 36, 65–89
24 Rosevear, F.B. (1954) J. Am. Oil Chem. Soc. 31, 628–639
25 Small, D.M. (1984) J. Lipid Res. 25, 1490–1500
26 Reiss-Husson, F. (1967) J. Mol. Biol. 25, 363–382
27 Ruocco, M.J., Shipley, G.G. and Oldfield, E. (1983) Biophys. J. 43, 91–101